Post-print of: Kozieł S., Bekasiewicz A.: Three-objective antenna optimization by means of kriging surrogates and domain segmentation. 2018 22nd International Microwave and Radar Conference (MIKON). DOI: 10.23919/MIKON.2018.8405222

Three-Objective Antenna Optimization By Means of Kriging Surrogates and Domain Segmentation

Slawomir Koziel[1,2]
[1]Engineering Optimization & Modeling Center
Reykjavik University
Reykjavik, Iceland
koziel@ru.is

Adrian Bekasiewicz[2]
[2]Faculty of Electronics, Telecommunications and Inf.
Gdansk University of Technology
Gdansk, Poland
bekasiewicz@ru.is

***Abstract*—In this paper, an optimization framework for multi-objective design of antenna structures is discussed which exploits data-driven surrogates, a multi-objective evolutionary algorithm, response correction techniques for design refinement, as well as generalized domain segmentation. The last mechanism is introduced to constrain the design space region subjected to sampling, which permits reduction of the number of training data samples required for surrogate model identification. The generalized segmentation technique works for any number of design objectives. Here, it is demonstrated using a three-objective case study of a UWB monopole optimized for best in-band reflection, minimum gain variability, and minimum size. The numerical results indicate that segmentation leads to reducing the cost of initial Pareto identification by around 21 percent as compared to the conventional surrogate-assisted approach.**

Keywords*—Antenna design; multi-objective optimization; EM-driven design; kriging interpolation; domain segmentation

I. INTRODUCTION

Design of contemporary antennas is a challenging process due to several factors, one of them being stringent performance specifications imposed on electrical and field properties of the structure at hand. Many of these requirements are conflicting, i.e., improving one of them leads to degradation of others. A typical example is design of compact wideband antennas, where reduction of the physical dimensions of the structure results in problems with achieving sufficient impedance bandwidth [1], increased gain variability or degradation of pulse stability [2]. On the practical side, handling multiple design goals is difficult and it is often realized in a simple manner, e.g., by selecting a primary objective and controlling others using implicit [3] or explicit constraints [4]. There are other reasons that make antenna design challenging, such as geometrical complexity (typically implying a large number of adjustable parameters), and necessity of using full-wave EM simulations for antenna evaluation, which is computationally expensive. Clearly, given the above challenges, simple design methods involving parameter sweeping normally fail to identify optimum designs.

Vast majority of reported design techniques and cases concern single-objective design. A typical situation is introduction of various topological alterations of the basic antenna structure and parameter tuning upon selecting the final topology. The tuning process is often oriented towards achieving a required impedance bandwidth whereas the values of other performance figures are not controlled explicitly (e.g., [5]-[7]). An improved control over multiple antenna characteristics can be achieved through numerical optimization [8]. Unfortunately, in many cases, conventional optimization algorithms [9] turn out to be prohibitively expensive. This particularly applies to population-based metaheuristics (genetic/evolutionary algorithms, particle swarm optimizers [10]-[12]). Design speedup can be obtained using adjoint sensitivities [13] or surrogate-based optimization (SBO) techniques [14]. The latter exploit faster representations of the structure under design either based on auxiliary data-driven models [15] or coarse-discretization EM simulations [14].

The most comprehensive information about the antenna structure and its capabilities in the context of a particular set of performance figures can be obtained by means of multi-objective optimization (MOO). The goal of MOO is to find a Pareto set which represents the best possible trade-offs between considered design objectives. The most popular MOO techniques up to date are population-based metaheuristics [11], [12]. Their principal advantage is the ability to generate the entire Pareto set in a single algorithm run [16]. All major metaheuristic algorithms have their multi-objective versions. A disadvantage is high computational cost (typically, thousands and tens of thousands of objective function evaluations are necessary for the algorithm to converge). Obviously, this translates into unacceptable costs if the antenna evaluation is performed using full-wave EM analysis.

Similarly as for single-objective optimization, the difficulties pertinent to high cost of MOO can be alleviated using surrogate-assisted methods. In [17], a technique involving variable-fidelity simulations and auxiliary kriging interpolation models has been proposed, further enhanced by means of design space reduction techniques [18], [19]. These methods are capable of yielding Pareto sets at the costs corresponding to only a few hundred evaluations of the high-fidelity EM simulations of the antenna structure at hand, and handling highly-dimensional cases (> 20 parameters). In [20], a design segmentation approach has been introduced in order to

reduce the number of samples necessary to construct the kriging surrogate model for the method [18], leading to further reduction of the CPU cost of MOO. Segmentation works by defining—based on appropriately defined intermediate points—a set of compartments that cover the Pareto front and the total volume of which is significantly smaller than that of the original design space. Unfortunately, the segmentation of [20] only works for two objectives. In this paper, the segmentation approach is generalized to an arbitrary number of objectives. Our technique is demonstrated using a three-objective case study of an ultra-wideband monopole antenna. The objectives are minimization of in-band reflection, minimization of gain variability, and reduction of the antenna size. Numerical results indicate that segmentation leads to 21-percent reduction of the cost of initial Pareto set identification.

II. Surrogate-Based Multi-Objective Optimization

The primary computational model used to evaluate performance of the antenna structure at hand is a high-fidelity EM simulation model $\boldsymbol{R}_f(\boldsymbol{x})$. Here, $\boldsymbol{x}$ is a vector of designable antenna parameters. The design problem is stated as simultaneous minimization of N_{obj} objectives $F_k(\boldsymbol{R}_f(\boldsymbol{x}))$, $k = 1, \ldots, N_{obj}$. Comparison of two designs $\boldsymbol{x}$ and $\boldsymbol{y}$ can be realized using a dominance relation $\prec$ defined as follows: $\boldsymbol{y} \prec \boldsymbol{x}$ (or $\boldsymbol{y}$ dominates over $\boldsymbol{x}$) if $F_k(\boldsymbol{R}_f(\boldsymbol{y})) \le F_k(\boldsymbol{R}_f(\boldsymbol{x}))$ for all $k = 1, \ldots, N_{obj}$, and $F_k(\boldsymbol{R}_f(\boldsymbol{y})) < F_k(\boldsymbol{R}_f(\boldsymbol{x}))$ for at least one k [16]. MOO aims at identifying a set X_P of Pareto-optimal designs (i.e., those that are not dominated by any other designs). The Pareto set represents the best possible trade-offs between objectives F_k.

The benchmark optimization approach is a methodology of [18]. It is a surrogate-based approach that exploits a coarse-discretization model $\boldsymbol{R}_{cd}$ and an auxiliary kriging interpolation model $\boldsymbol{R}_s$. It can be summarized as follows:

1. Design space reduction. Set the lower/upper bounds of the design space X_0 as $\boldsymbol{l} = \min\{\boldsymbol{x}^{*(1)}, \boldsymbol{x}^{*(2)}, \ldots, \boldsymbol{x}^{*(N_{obj})}\}$ and $\boldsymbol{u} = \max\{\boldsymbol{x}^{*(1)}, \boldsymbol{x}^{*(2)}, \ldots, \boldsymbol{x}^{*(N_{obj})}\}$, where $\boldsymbol{x}^{*(k)} = \operatorname{argmin}\{\boldsymbol{x} : F_k(\boldsymbol{R}_{cd}(\boldsymbol{x}))\}$ are extreme Pareto-optimal designs obtained through single-objective optimization runs.
2. Surrogate model construction. Allocate training data samples within X_0, acquire $\boldsymbol{R}_{cd}$ simulation data, and identify kriging interpolation model $\boldsymbol{R}_s$.
3. Obtaining initial Pareto set. Optimize $\boldsymbol{R}_s$ using multi-objective evolutionary algorithm (MOEA) [18].
4. Design refinement. Select K designs $\boldsymbol{x}_s^{(k)}$, $k = 1, \ldots, K$; obtain high-fidelity-level design $\boldsymbol{x}_f^{(k)}$ as

$$\boldsymbol{x}_f^{(k)} = \arg \min_{\substack{\boldsymbol{x},\ F_2(\boldsymbol{x}) \le F_2(\boldsymbol{x}_s^{(k)}) \\ \vdots \\ F_{N_{obj}}(\boldsymbol{x}) \le F_{N_{obj}}(\boldsymbol{x}_s^{(k)})}} F_1\left(\boldsymbol{R}_s(\boldsymbol{x}) + [\boldsymbol{R}_f(\boldsymbol{x}_s^{(k)}) - \boldsymbol{R}_s(\boldsymbol{x}_s^{(k)})]\right) \quad (1)$$

Procedure (1) can be iterated; typically 2-3 iterations are sufficient for convergence.

The above algorithm permits low-cost MOO (optimization cost typically corresponds to a few hundred of high-fidelity model evaluations [17], [18]). Further cost reduction can be achieved by domain segmentation briefly discussed and generalized in Section III.

III. Generalized Design Space Segmentation

The original concept of design space segmentation (defined for two-objective case) has been illustrated in Fig. 1(a). Given $\boldsymbol{d}^{(1)} = [d_1^{(1)}\ d_2^{(1)}\ \ldots\ d_n^{(1)}]^T = |\boldsymbol{x}^{*(1)} - \boldsymbol{x}^{*(2)}|$ (the size vector of the design space X_0), the volume of X_0 is $V_0 = \prod_{k=1,\ldots,n} d_k^{(1)}$. By introducing one intermediate point $\boldsymbol{x}_I^{(1)}$, two reduced sub-domains are created, $X_{1.1}$ and $X_{1.2}$ with the volumes of $V_{1.I} = \prod_{k=1,\ldots,n} d_k^{(I.I)}$, where $\boldsymbol{d}^{(I.1)} = [d_1^{(I.1)}\ \ldots\ d_n^{(I.1)}]^T = |\boldsymbol{x}^{*(1)} - \boldsymbol{x}_I^{(1)}|$, and $\boldsymbol{d}^{(I.2)} = [d_1^{(I.2)}\ \ldots\ d_n^{(I.2)}]^T = |\boldsymbol{x}^{*(2)} - \boldsymbol{x}_I^{(1)}|$. The intermediate point is obtained as

$$\boldsymbol{x}_I^{(1)} = \arg \min_{\boldsymbol{x},\ F_2(\boldsymbol{x}) \le F_{2.I}^{(1)}} F_1\left(\boldsymbol{R}_{cd}(\boldsymbol{x})\right) \quad (2)$$

where the threshold $F_{2.I}^{(1)}$ is set to place the intermediate point around the middle of the Pareto front, i.e., $F_{2.I}^{(1)} = [F_2(\boldsymbol{x}^{*(1)}) + F_2(\boldsymbol{x}^{*(2)})]/2$. The cost of finding $\boldsymbol{x}_I^{(1)}$ is low because the starting point $[\boldsymbol{x}^{*(1)} + \boldsymbol{x}^{*(2)}]/2$ provides its good approximation (assuming low curvature of the Pareto front, which is usually the case of antenna design problems).

In a general two-objective case, K intermediate points $\boldsymbol{x}_I^{(l)}$, $l = 1, \ldots, K$, are created along with $K + 1$ sub-domains $X_{K.l}$, $l = 1, \ldots, K + 1$ of the volumes $V_{K.l} = \prod_{k=1,\ldots,n} d_k^{(I.l)}$, where $\boldsymbol{d}^{(I.1)} = |\boldsymbol{x}^{*(1)} - \boldsymbol{x}_I^{(1)}|$, $\boldsymbol{d}^{(I.l)} = |\boldsymbol{x}_I^{(l-1)} - \boldsymbol{x}_I^{(l)}|$ for $l = 2, \ldots, K$, and $\boldsymbol{d}^{(I.K+1)} = |\boldsymbol{x}^{*(2)} - \boldsymbol{x}_I^{(K)}|$. We have $\boldsymbol{x}_I^{(l)} = \operatorname{argmin}\{\boldsymbol{x} : F_1(\boldsymbol{R}_{cd}(\boldsymbol{x})),\ F_2(\boldsymbol{x}) \le F_{2.I}^{(l)}\}$, where $F_{2.I}^{(l)} = (1 - \alpha_l)F_2(\boldsymbol{x}^{*(1)}) + \alpha_l F_2(\boldsymbol{x}^{*(2)})$, $\alpha_l = l/K$.

The fundamental benefit of segmentation is that the total volume $V_K = V_{K.1} + \ldots + V_{K.K+1}$ is much smaller than V_0 (cf. [20] for details) so that the overall number of training samples necessary to build the kriging model (set up independently for each segment) is smaller than in case of constructing the model in X_0. According to [20], increasing the number of segments makes these benefits more pronounced but they are counterweighted by the increasing cost of finding the intermediate points. In practice, selecting one or two intermediate points seems to be optimal for typical two-objective antenna problems.

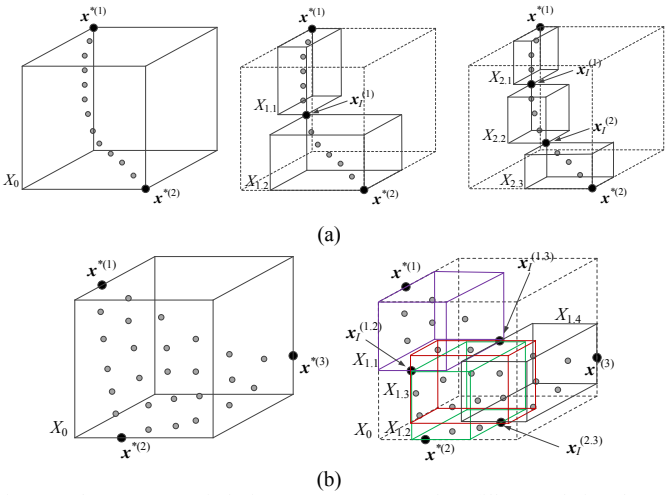

Fig. 1. The concept of design space segmentation (illustrated for three-dimensional design space): (a) two design objectives: three cases shown with no segementation, two-fold, and three-fold segmentation, (b) three design objectives: two cases shown with no segmentation and two-fold segmentation. The overall volume of the segments is smaller than the volume of the original space and the benefits increase with the number of segments. Generalization for higher number of objectives is straightforward.

Figure 1(b) illustrates segmentation for a three-objective case. Here, for two-fold segmentation, one needs three intermediate points $\boldsymbol{x}_I^{(1.2)}$, $\boldsymbol{x}_I^{(1.3)}$, $\boldsymbol{x}_I^{(2.3)}$, which results in four segments covering the entire Pareto set. The points are obtained as ($k, j = 1, 2, 3, k < j$)

$$\boldsymbol{x}_I^{(k.j)} = \arg \min_{\boldsymbol{x},\, F_j(\boldsymbol{x}) \le F_{j.I}^{(1)}} F_k\left(\boldsymbol{R}_{cd}(\boldsymbol{x})\right) \tag{3}$$

Note that the intermediate points are obtained by optimizing one of the objectives with constraints imposed on the second while disregarding the third one. This way, one can relocate the intermediate points to the boundaries of the Pareto front. Three-fold (and higher-order) segmentation can be defined analogously. We omit details here because of complexity of notation involved. In a similar way, one can define segmentation for a larger number of objectives. In case of four objectives, two-fold segmentation has four intermediate points and five segments.

IV. Demonstration Example and Results

The concept of generalized segmentation is demonstrated using a UWB monopole antenna with two radiator slots and an elliptical slit below the feed line shown in Fig. 2 [21]. The antenna is implemented on FR4 substrate ($\varepsilon_r = 4.3$, $h = 1.55$ mm). The design parameters are $\boldsymbol{x} = [L_g\ L_0\ L_s\ W_s\ d\ dL\ d_s\ dW_s\ dW\ a\ b]^T$; $W_0 = 2.0$. The unit for all dimensions is mm. The EM antenna models are implemented in CST Microwave Studio [22] ($\boldsymbol{R}_f$: ~2,200,000 mesh cells, simulation time 15 minutes, and $\boldsymbol{R}_c$: ~160,000 cells, 40 seconds); the SMA connector to ensure reliability of antenna evaluation. We consider three objectives: F_1 – minimization of reflection in 3.1 GHz to 10.6 GHz band, F_2 – minimization of antenna footprint (defined as $A(\boldsymbol{x}) = (2dW + 2dW_s + 2W_s + d)(L_0 + 2d_s + L_s + dL)$), and F_3 – minimization of realized gain variability within UWB frequency range. Furthermore, we are only interested in designs for which the maximum in-band reflection does not exceed–10 dB.

The extreme Pareto-optimal designs have been found using trust-region gradient search. These are $\boldsymbol{x}_1^* = [8.86\ 12.96\ 9.39\ 0.35\ 3.89\ 6.46\ 1.22\ 1.58\ 2.58\ 0.33\ 0.55]^T$, $\boldsymbol{x}_2^* = [9.27\ 13.20\ 8.90\ 0.25\ 3.29\ 0.00\ 0.70\ 1.46\ 0.72\ 0.67\ 0.61]^T$, and $\boldsymbol{x}_3^* = [8.38\ 12.82\ 9.89\ 0.65\ 3.84\ 14.99\ 1.54\ 1.68\ 2.65\ 0.39\ 0.55]^T$. Consequently, the lower/upper bounds of X_0 are $\boldsymbol{l}^* = [8.38\ 12.82\ 8.9\ 0.25\ 3.29\ 0.0\ 0.7\ 1.46\ 0.72\ 0.33\ 0.55]^T$ and $\boldsymbol{u}^* = [9.27\ 13.2\ 8.89\ 0.65\ 3.89\ 14.99\ 1.54\ 1.68\ 2.65\ 0.67\ 0.61]^T$.

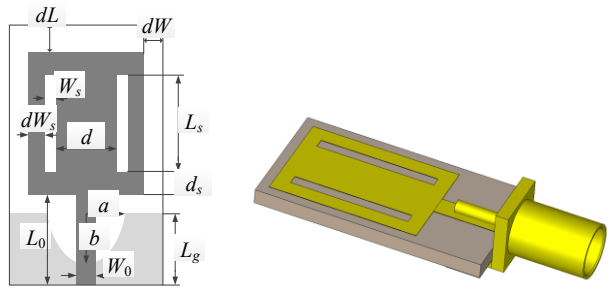

(a) (b)

Fig. 2. UWB monopole antenna with elliptical slit below the feed line: (a) top view, (b) 3D view. The ground plane marked with light-gray shade.

The three intermediate points have then been obtained using (3) as follows: $\boldsymbol{x}_I^{(1.2)} = [9.12\ 13.04\ 8.79\ 0.29\ 3.43\ 2.91\ 0.87\ 1.38\ 1.48\ 0.53\ 0.57]^T$, $\boldsymbol{x}_I^{(1.3)} = [8.72\ 12.8\ 9.53\ 0.51\ 3.95\ 11.36\ 1.33\ 1.61\ 2.5\ 0.35\ 0.54]^T$, $\boldsymbol{x}_I^{(2.3)} = [8.8\ 12.99\ 9.42\ 0.45\ 3.59\ 7.25\ 1.1\ 1.57\ 1.6\ 0.54\ 0.57]^T$. The ratio of the volume V_0 of X_0 and the combined volume V_1 of the four segments $X_{1.j}$ (cf. Fig. 1(b)) is around 10^2. The kriging model $\boldsymbol{R}_s$ constructed in X_0 requires 843 data samples (average RMS error of 2.5 percent). The total number of samples required to establish the kriging models in $X_{1.j}$ is 103 + 83 + 63 + 123 = 372 (average errors of 2.4, 2.5, 2.1, and 2.5 percent, respectively). This represents noticeable savings.

Figure 3 shows the initial Pareto set obtained by optimizing the kriging surrogate using MOEA (Step 3 of the MO procedure of Section II) as well as the Pareto set found in the segmented space. The latter is obtained by selecting the non-dominated designs from the concatenated Pareto sets obtained in all segments. It can be observed that the representations are similar to one another which indicates that segmentation does not result in Pareto front quality degradation. At the same time, the cost of MO is smaller when using design segmentation as indicated in Table I.

Figure 4 shows the final (high-fidelity) Pareto set obtained using the methodology of Section II with design segmentation. Table II gathers antenna dimensions for high-fidelity Pareto-optimal designs. Reflection and realized gain responses for the selected designs have been shown in Figs. 4 and 5.

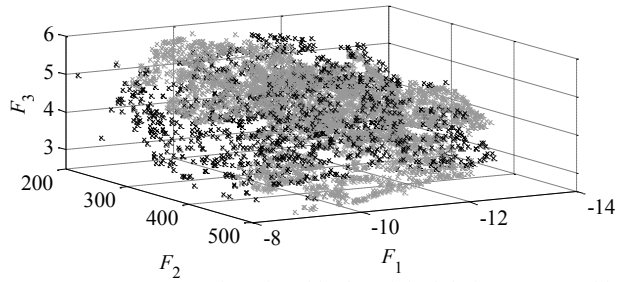

Fig. 3. Pareto set representations found in the original design space X_0 (black) and in the segmented space (gray).

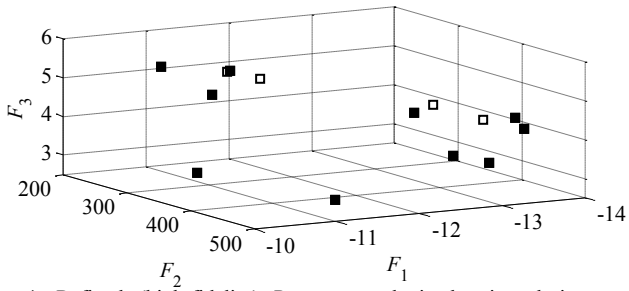

Fig. 4. Refined (high-fidelity) Pareto set obtained using design space segmentation. Designs marked using filled squares are listed in Table II.

TABLE I Multi-Objective Optimization Cost Breakdown

Cost contributor	No segmentation	Two-fold segmentation
Extreme and intermediate points	347 $\boldsymbol{R}_{cd}$	569 $\boldsymbol{R}_{cd}$
Data acquisition	843 $\boldsymbol{R}_{cd}$	372 $\boldsymbol{R}_{cd}$
MOEA optimization	N/A	N/A
Refinement	45 $\boldsymbol{R}_f$	45 $\boldsymbol{R}_f$
Total cost	97.9 $\boldsymbol{R}_f$ (24.5 h)	86.8 $\boldsymbol{R}_f$ (21.7 h)

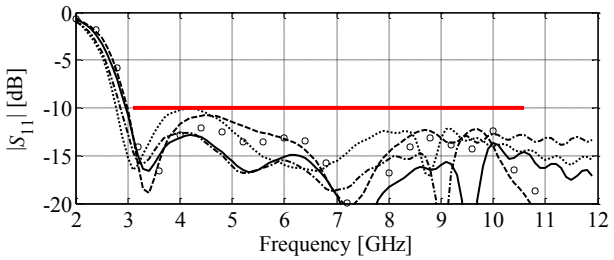

Fig. 5. Reflection responses of the selected high-fidelity Pareto-optimal designs (cf. Table II): $\boldsymbol{x}_f^{(1)}$ (····), $\boldsymbol{x}_f^{(3)}$ (–·–), $\boldsymbol{x}_f^{(5)}$ (– –), $\boldsymbol{x}_f^{(7)}$ (—),$\boldsymbol{x}_f^{(9)}$ (○○).

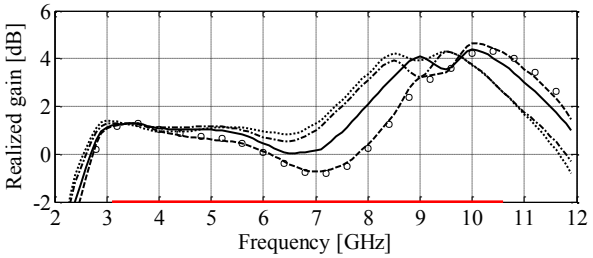

Fig. 6. Realized gain responses of the selected high-fidelity Pareto-optimal designs (cf. Table II): $\boldsymbol{x}_f^{(1)}$ (····), $\boldsymbol{x}_f^{(3)}$ (–·–), $\boldsymbol{x}_f^{(5)}$ (– –), $\boldsymbol{x}_f^{(7)}$ (—),$\boldsymbol{x}_f^{(9)}$ (○○).

TABLE II HIGH-FIDELITY PARETO-OPTIMAL DESIGNS

	Pareto-optimal design									
	$\boldsymbol{x}^{(1)}$	$\boldsymbol{x}^{(2)}$	$\boldsymbol{x}^{(3)}$	$\boldsymbol{x}^{(4)}$	$\boldsymbol{x}^{(5)}$	$\boldsymbol{x}^{(6)}$	$\boldsymbol{x}^{(7)}$	$\boldsymbol{x}^{(8)}$	$\boldsymbol{x}^{(9)}$	$\boldsymbol{x}^{(10)}$
F_1	–10.1	–13.7	–12.6	–11.0	–10.8	–12.9	–12.9	–11.0	–11.5	–13.7
F_2	400	428	476	298	253	497	380	496	261	446
F_3	3.5	4.3	3.7	4.8	5.4	3.6	4.4	3.0	5.1	4.1
L_g	8.60	9.00	8.77	8.90	9.14	8.80	8.93	8.57	9.19	9.07
L_0	12.81	12.92	12.85	12.88	13.07	12.84	12.83	12.88	13.02	12.94
L_s	9.86	9.22	9.53	9.15	9.26	9.47	8.92	9.64	8.99	9.15
W_s	0.57	0.43	0.58	0.44	0.36	0.52	0.50	0.61	0.39	0.51
d	3.85	3.71	3.83	3.62	3.50	3.88	3.84	3.89	3.53	3.75
dL	8.44	9.31	11.61	2.91	1.86	12.67	7.93	13.76	2.30	11.25
d_s	1.34	1.09	1.14	1.29	0.79	1.10	0.95	1.38	0.72	1.08
dW_s	1.63	1.56	1.64	1.60	1.46	1.64	1.56	1.64	1.49	1.52
dW	1.80	2.51	2.43	1.57	1.33	2.58	2.03	2.16	1.42	2.38
a	0.44	0.35	0.36	0.44	0.55	0.35	0.44	0.37	0.53	0.38
b	0.56	0.55	0.56	0.56	0.59	0.56	0.55	0.56	0.60	0.55

V. CONCLUSION

In the paper, a generalized design space segmentation technique for accelerated multi-objective optimization of antennas has been discussed. Our approach allows for reducing the number of training data samples necessary to establish the kriging surrogate model, thus leading to the lower overall optimization cost. The proposed method has been demonstrated using a UWB monopole antenna with three design objectives concerning reflection response, realized gain, and the structure footprint. For this case study, space segmentation results in lowering the cost of initial Pareto set generation by 21 percent.

ACKNOWLEDGMENT

The authors would like to thank Computer Simulation Technology AG, Darmstadt, Germany, for making CST Microwave Studio available. This work was supported in part by the Icelandic Centre for Research (RANNIS) Grant 163299051, and by National Science Centre of Poland Grant 2015/17/B/ST6/01857.

REFERENCES

[1] S. Nikolaou and M. A. B. Abbasi, "Design and development of a compact UWB monopole antenna with easily-controllable return loss," *IEEE Trans. Ant. Propag*., vol. 65, no. 4, pp 2063-2067, 2017.

[2] J. Liu, K.P. Esselle, S.G. Hay, and S. Zhong, "Effects of printed UWB antenna miniaturization on pulse fidelity and pattern stability," *IEEE Trans. Ant. Prop.*, vol. 62, no. 8, pp 3903-3910, 2014.

[3] A. Bekasiewicz and S. Koziel, "Structure and computationally-efficient simulation-driven design of compact UWB monopole antenna," *IEEE Antennas and Wirel. Propag. Lett*., vol. 14, pp. 1282–1285, 2015.

[4] M.A. Haq and S. Koziel, "A novel miniaturized uwb monopole with five-section stepped-impedance feed line," *Microwave Opt. Tech. Lett.*, 2017.

[5] L. Li, S.W. Cheung, and T.I. Yuk, "Compact MIMO antenna for portable devices in UWB applications," *IEEE Trans. Antennas Prop.*, vol. 61, no. 8, pp. 4257–4264, 2013.

[6] M. N. Shakib, M. Moghavvemi, and W. N. L. Mahadi, "Design of a compact planar antenna for ultra-wideband operation," *Applied Computational Electromagnetics Society Journal*, vol. 20, no. 2, pp 222-229, 2015.

[7] M. Manohar, R. S. Kshetrimayum, and A. K. Gogoi, "Printed monopole antenna with tapered feed line, feed region and patch for super wideband applications," *IET Microw. Antennas propag*., vol. 8, Iss. 1, pp 39-45, 2014.

[8] B. Tian, Z. Li, C. Wang, "Boresight gain optimization of an UWB monopole antenna using FDTD and genetic algorithm," *IEEE Int. Conf. Ultra-Wideband*, pp. 1-4, 2010.

[9] J. Nocedal, S.J. Wright, *Numerical Optimization*, Springer, 2006.

[10] X.-S. Yang, K.-T. Ng, S.H. Yeung, and K.F. Man, "Jumping genes multiobjective optimization scheme for planar monopole ultrawideband antenna," *IEEE Trans. Antennas Prop.*, vol. 56, no. 12, pp. 3659-3666, 2008.

[11] D. Ding and G. Wang, "Modified multiobjective evolutionary algorithm based on decomposition for antenna design," *IEEE Trans. Antennas Prop.*, vol. 61, no. 10, pp. 5301-5307, Oct. 2013.

[12] S. Chamaani, S.A. Mirtaheri, and M.S. Abrishamian, "Improvement of time and frequency domain performance of antipodal Vivaldi antenna using multi-objective particle swarm optimization," *IEEE Trans. Antennas Prop.*, vol. 59, no. 5 pp. 1738-1742, May 2011.

[13] M. Ghassemi, M. Bakr, and N. Sangary, "Antenna design exploiting adjoint sensitivity-based geometry evolution," *IET Microwaves Ant. Prop.*, vol. 7, no. 4, pp. 268-276, 2013.

[14] S. Koziel, and S. Ogurtsov, *Antenna design by simulation-driven optimization*, Springer, New York, 2014.

[15] N.V. Queipo, R.T. Haftka, W. Shyy, T. Goel, R. Vaidynathan, and P.K. Tucker, "Surrogate-based analysis and optimization," *Prog. Aerospace Sci.*, vol. 41, no. 1, pp. 1-28, Jan. 2005.

[16] K. Deb., *Multi-objective optimization using evolutionary algorithms*, New York: John Wiley & Sons, 2001.

[17] S. Koziel and S. Ogurtsov, "Multi-objective design of antennas using variable-fidelity simulations and surrogate models," *IEEE Trans. Antennas Prop.*, vol. 61, no. 12, pp. 5931-5939, Dec. 2013.

[18] S. Koziel, and A. Bekasiewicz, "Low-cost multi-objective optimization and experimental validation of UWB MIMO antenna," *Eng. Comp.*, vol. 33, no. 4, pp. 1246-1268, 2016.

[19] S. Koziel and A. Bekasiewicz, "Computationally efficient two-objective optimization of compact microwave couplers through corrected domain patching," *Metrology and Measurement Systems*, 2017.

[20] S. Koziel, A. Bekasiewicz, Q.S. Cheng, and S. Li, "Accelerated multi-objective design optimization of antennas by surrogate modeling and domain segmentation," *IEEE European Ant. Prop. Conf.*, 2017.

[21] M.A. Haq, S. Koziel, and Q.S. Cheng, "EM-driven size reduction of UWB antennas with ground plane modifications," *Int. Applied Computational Electromagnetics Society (ACES China) Symposium*, 2017.

[22] CST Microwave Studio, ver. 2016. CST AG, Bad Nauheimer Str. 19, D-64289 Darmstadt, Germany, 2016.